



0191-2615(95)00004-6

## A FINITE DIFFERENCE APPROXIMATION OF THE KINEMATIC WAVE MODEL OF TRAFFIC FLOW

CARLOS F. DAGANZO

Department of Civil Engineering and Institute of Transportation Studies, University of California, Berkeley CA 94720 U.S.A.

(Received 3 November 1993; in revised form 1 November 1994)

**Abstract**— This article shows that if the kinematic wave model of freeway traffic flow in its general form is approximated by a particular type of finite difference equation, the finite difference results converge to the kinematic wave solution despite the existence of shocks in the latter. This result, which applies to initial and boundary condition problems with and without discontinuous data, is shown not to hold for other commonly used finite difference schemes. In the proposed approximation, the flow between two neighboring lattice points is the minimum of the two values returned by: (a) a “sending” function evaluated at the density prevailing at the upstream lattice point and (b) a “receiving” function evaluated at the downstream lattice point. The sending and receiving functions correspond to the increasing and decreasing branches of the freeway’s flow-density curve. The article presents an asymptotic formula for the errors introduced by the proposed finite difference approximation and describes quantitatively the finite difference’s shock-capturing behavior. Errors are shown to be approximately proportional to the mesh spacing with a coefficient of proportionality that depends on the wave speed, on its rate of change with density, and on the slope and curvature of the initial density profile. The asymptotic errors are smaller than those of Lax’s first-order, centered difference method which is also convergent. More importantly though, the proposed procedure never yields negative flows, and this makes it attractive in practical engineering applications when the mesh cannot be made arbitrarily small.

### 1. INTRODUCTION

In the belief that the behavior of freeway traffic at a given point in time-space is only affected by the state of the system in a neighborhood of that point some researchers have examined the possibility of representing traffic phenomena by partial differential equations (PDEs). Most notable among these efforts are: the first order model of Light-hill and Whitham (1955) and Richards (1956) (the LWR model), the first order systems of Bick and Newell (1960) for two-lane bidirectional roads, and Munjal and Pipes (1971) for multilane freeways and the higher order model of Payne (1971). In the same spirit, other researchers have proposed systems of finite difference equations (FDEs) to model freeway traffic, often claiming to approximate one of the aforementioned PDEs (e.g., Payne, 1979; Michalopoulos et al., 1984, 1984a; Cremer & May, 1985).

For PDE and FDE models, one should expect small perturbations to the initial conditions of the system (disturbances) to propagate forward when traffic is light, backward when traffic is heavy, and never to travel faster than the vehicle(s) that caused it. This happens for the LWR model, which is the focus of this article but not for every model that has been proposed. An understanding of the propagation of disturbances is also important in the development of solution methods. As we shall see, the existence of disturbances that can travel either upstream or downstream in the LWR model (but not in both directions simultaneously as would occur for second order PDEs) invalidates many numerical approaches that on first sight might seem reasonable; e.g., it invalidates any forward differencing scheme but not the centered differencing method (Lax, 1954) used in Michalopoulos et al. (1984).

The development of discontinuities (or shocks) in the LWR model, even when the initial conditions are smooth, also creates difficulties. This article shows that despite these complicating features, a specific FDE approximation to the LWR model exists, which never yields negative flows, can be run across shocks, and tends to the LWR solution as the lattice spacing is reduced.

As a prelude to our discussion and to make the paper self-contained, a brief review of the LWR model is presented in Section 2. The new material starts with the treatment of a highway that is homogeneous in time and space in Sections 3 and 4. Section 3 describes the proposed FDE and shows that the solution depends on initial conditions in a way that properly captures two-way propagation of disturbances; the logic leads to an intuitive proof of convergence and an error formula for a particular form of the LWR model. The article then examines the general case using different arguments: Section 4 presents an asymptotic error formula for the predictions and Section 5 a formula for the FDE shock profile which describes quantitatively its shock-capturing behavior. Finally, Sections 6 and 7 discuss possible extensions and present some conclusions.

## 2. THE LWR MODEL

If no net flow enters a highway, vehicle conservation induces a relation between the rates of change of flow ( $q$ ) with respect to space ( $x$ ) and density ( $k$ ) with respect to time ( $t$ ). Using subscripts  $t$  and  $x$  to denote partial derivatives with respect to time and space, the relation can be expressed as follows:

$$q_x + k_t = 0. \quad (1)$$

The LWR theory assumes that in addition to (1) flow and density are also related by a continuous and piecewise differentiable equation of state at all points in time-space:

$$q = S(k, x, t). \quad (2)$$

Lighthill and Whitham (1955) analyzed in detail the case where (2) was independent of  $t$ .

### 2.1. Solution methods

Given an equation of state  $q = S(k, x, t)$  and a well-posed set of initial/boundary conditions (e.g., given a smooth, slow-varying  $k(x, 0)$  that is defined for all  $x$ ), it is possible to determine  $k(x, t)$  everywhere except on curves (called shockpaths) where  $k(x, t)$  is discontinuous.

A conventional method of solution for the LWR model uses the method of characteristics. A characteristic is a curve (with space as a function of time) that emanates from a time-space point where the initial conditions are known, with the property that the traffic density along the curve does not change if  $k(x, t)$  is perturbed at any points (initial or otherwise) not on the curve. As such, characteristics can be viewed as *causality lines* which indicate which points in time-space influence which others. It is clear from their defining property that characteristic curves cannot intersect. If they meet they must terminate at the meeting point, where a shock arises.

For equations of the type defined by (1) and (2)—where the latter varies in time and space—with a well-posed set of initial/boundary conditions, a family of characteristic curves exists which spans the whole space; i.e., every point not on a shock is reached from exactly one characteristic that extends backward in time to some initial or boundary point.

This means that the density at every point (as well as any conditions related to density, such as flow and speed) can be traced backward in time to some location on the initial/boundary region, and that small disturbances on the initial/boundary region outside that location cannot influence those conditions. (This is true as long as the disturbances are small; otherwise, the disturbances could change the position of the shocks so much that the point of interest might switch characteristics.) It follows that if an infinitesimal increase in density (a disturbance) occurs at any point it must propagate along the characteristic curve passing through that point without affecting points lying on other characteristics. Characteristic curves, thus, define the paths of disturbances.

To find the characteristics, replace  $q$  by  $S(k, x, t)$  in (1), which yields:

$$k_t + k_x S_k = -S_x. \quad (3)$$

Because the left-hand side is the directional derivative of  $k$  in the direction  $(1, S_k)$  in the  $(t, x)$  plane, the slope of the characteristic (also termed the *wave-speed*) is:

$$dx/dt = S_k, \quad (4a)$$

and the density's growth rate along the characteristic is:

$$dk/dt = -S_x. \quad (4b)$$

For a heterogeneous highway  $S_k$  and  $S_x$  are functions of density and space as well as time. Thus, the characteristics are curves that are found by solving the system of ordinary differential equations (4); e.g., by stepping through time in small increments.

For a homogeneous highway in time and space  $S_x$  is zero. It then follows from (4b) that the characteristics must be curves of constant density (and flow). Because  $S_k$  is then constant along the curve, (4a) implies that the characteristics must be straight lines.

The solution method is not complete without specifying a rule for the location of shocks. This prevents points from being reached by more than one characteristic. In the traditional solution method, one normally specifies, based on the continuity equation, a condition for the speed of a shock  $U$  separating a neighborhood of points with density-flow  $(k^a, q^a)$  from points with density-flow  $(k^b, q^b)$ :

$$U = (q^b - q^a)/(k^b - k^a). \quad (5)$$

This condition is sufficient (for well-posed problems) to define uniquely the location of all shocks although the solution methods are laborious. This is discussed extensively in Lighthill and Whitham (1955).

Because characteristics must reach back to the initial data, note that the only types of shocks that can be present in the solution are those where the characteristics converge into the shock. For  $S(k, x, t)$  relations that are strictly concave in  $k$  this means that shocks must be positive jumps in density as  $x$  increases.

If shocks are present in the initial data the problem does not necessarily become ill-posed; the shock simply propagates into the solution. However, if the initial data includes jumps that would cause the characteristics to diverge from the discontinuity (e.g., negative jumps for concave  $S$ ), one must treat these in some appropriate way. If  $S$  is concave in  $k$ , one simply introduces a fan of characteristics, as if the jump was the limiting form of a rapidly varying, smooth and monotonic function. (A combination of fans and shocks may be necessary if  $S$  is not concave.)

Luke (1972) presents a minimum principle that simplified the solution of certain classes of kinematic wave problems. Newell (1993) independently rediscovered this minimum principle and showed that it could be applied to a function  $N(x, t)$ , whose derivatives are  $q(x, t)$  and  $-k(x, t)$ . The method is exact and applies to concave or convex  $S$ . Newell (1993) also described an elegant simplification that allows graphical solution by hand (or computer) in the special case where the equation of state is triangular or trapezoidal. For the same special case, Daganzo (1994) presented a FDE method, termed the cell-transmission model, that approximates the PDE on a lattice even when the solution to the latter includes shocks and waves that can propagate in either direction. This method has been extended to general networks (Daganzo, 1995).

We propose here to generalize the cell-transmission FDE to arbitrary equations of state. The homogeneous highway is examined first. The following section presents the proposed FDE, shows how it depends on initial conditions and examines its convergence properties in a special case. It also shows that other FDEs fail to converge.

## 3. A PROPOSED FDE APPROXIMATION

As is customary we assume that the highway has been partitioned into sections or cells " $i$ " of length  $d_i$ , where  $i$  is an integer that increases by 1 across contiguous sections in the direction of advancing traffic and that it is observed every  $\epsilon$  time units. Because for a homogeneous highway  $S$  no longer depends on  $x$  and  $t$ , these two arguments will be dropped from our notation; i.e., we will write  $S(k)$  instead of  $S(k, x, t)$ , although we will continue to use  $k$  as a subscript to denote the derivatives of  $S$ . For a homogeneous highway the free-flow speed is a constant  $v^f = S_k(0)$  and we assume that  $d_i = d \geq v^f \epsilon$ . It will be shown later that this condition is needed for convergence and that the algorithm is most accurate if  $d = v^f \epsilon$ , as recommended in Daganzo (1994).

We define  $n(x, t)$  to be an occupancy function that at the lattice points ( $x = di$ ,  $t = \tau\epsilon$ , where  $i$  and  $\tau$  are integers) equals the occupancy of the corresponding cell at the specified instant of time. We also define  $y(x, t)$  to be a departure function that at the lattice points gives the number of vehicles that leave cell  $i = x/d$  between  $t$  and  $t + \epsilon$ . In time-space regions where the density is smooth the occupancy and departure functions are related to density and flow by:

$$n = kd \text{ and } y = q\epsilon, \text{ as } (d, \epsilon) \rightarrow 0.$$

Conservation requires that the following be satisfied at the lattice points:

$$n(x, t + \epsilon) = n(x, t) + y(x - d, t) - y(x, t). \quad (6a)$$

To simplify the notation we will use as unknown a density function,  $K(x, t) = n(x, t)/d$ , and an (exit) flow function,  $Q(x, t) = y(x, t)/\epsilon$ , so that the above expression becomes:

$$K(x, t + \epsilon)/\epsilon = K(x, t)/\epsilon - [Q(x, t) - Q(x - d, t)]/d \quad (6b)$$

As  $(\epsilon, d) \rightarrow 0$ , Eqs. (6b) and (1) become equivalent.

Equations (6) are exact; the FDE approximation is made when the equation of state is used to relate  $K$  and  $Q$ . Unfortunately, the seemingly natural form of expressing the relation:

$$Q(x, t) = S(K(x, t)), \quad (7a)$$

has some undesirable properties (Newell, 1989).

This can be easily seen if one expresses the FDE recursion in terms of  $K$  alone:

$$K(x, t + \epsilon)/\epsilon = K(x, t)/\epsilon - [S(K(x, t)) - S(K(x - d, t))]/d$$

and notes that conditions at  $x$  are only influenced by (upstream) conditions at  $x$  and  $x - d$ . This is graphically illustrated by the influence diagram of Fig. 1A, in which arrows denote causality. Clearly any initial conditions downstream of  $x$  have no impact on the conditions at the point of interest ( $P$ ), and the effects of this feature are disastrous: the FDE may pump traffic into a region at jam density and will also prevent stopped traffic from advancing into an empty region.

If conditions in the  $(t, x)$  region displayed in Fig. 1A are congested, the LWR characteristic passing through  $P$  will slant down so that conditions at  $P$  are determined from the conditions at  $Q$  and beyond. This would suggest replacing (7a) under congested conditions by:

$$Q(x, t) = S(K(x + d, t)), \quad (7b)$$

which results in a FDE recursion that only involves downstream conditions. The resulting influence diagram is displayed in Fig. 1B.

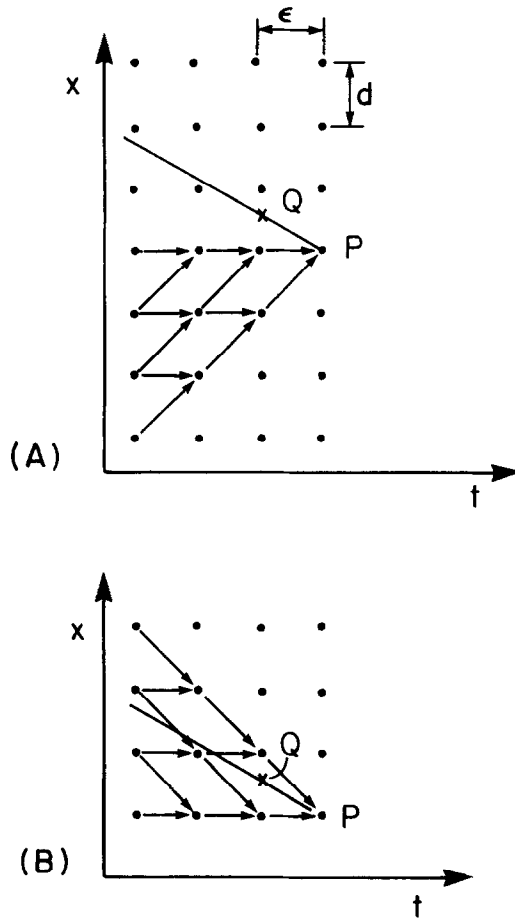


Fig. 1. Influence diagrams for the FDE.

Whereas (7b) has the potential for approximating the LWR solution when traffic is congested, it is clearly inadequate when traffic is uncongested and characteristics slope upward. The reverse occurs with (7a). Thus, here we propose to combine (7a) and (7b) into a single expression which will exhibit an influence diagram as in Fig. 1A under uncongested conditions and as in Fig. 1B under congested conditions.

Before presenting the proposed revision, we note that the customary (i.e., unimodal, continuous, and piecewise differentiable) form of (2) can be expressed as follows:

$$q = \min [T(k), R(k^j - k)] \quad (8)$$

where  $k^j$  represents the jam (maximum) density, and  $T$  and  $R$  are continuous, piecewise differentiable, nondecreasing functions defined in the interval  $[0, k^j]$  and such that  $T(0) = R(0) = 0$ ; see Fig. 2. These properties of  $S$ ,  $T$ , and  $R$  are taken as assumptions in this article.

For the proposed FDE approach to work, we must also assume that the speeds of forward and backward disturbances,  $T'$  and  $R'$ , are bounded from above. For simplicity of notation we assume here that this bound is the free flow speed,  $T'(0) = v^f$ , because this is reasonable for traffic modeling. (For other applications, the specific bound should replace  $v^f$  in the arguments and formulas presented next.)

We will use  $k^o$  to denote a density where the two terms of (8) are equal, and  $q^o$  the corresponding (maximum) flow. We define  $T(k)$  to be equal to  $q^o$  if  $k \geq k^o$ , and  $R(k^j - k) = q^o$  if  $k < k^o$ .

For the rest of this section we assume that the relationship between  $q$  and  $k$  is

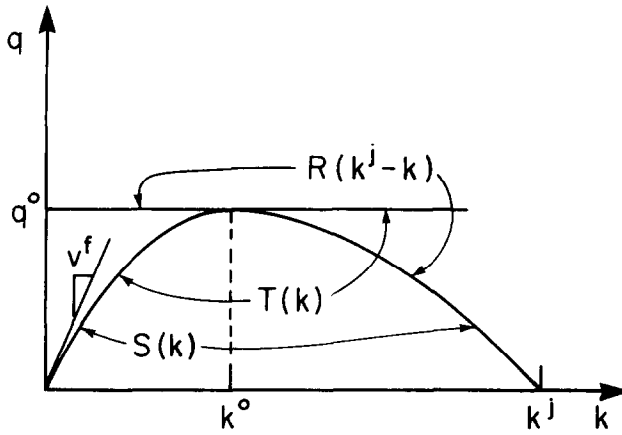


Fig. 2. Representation of the equation of state.

differentiable in  $[0, k^j]$ ; the generalization to piecewise differentiable forms is discussed later.

Our proposed FDE can now be stated. It approximates flows by:

$$Q(x, t) = \min\{T(K(x, t)), R(k^j - K(x + d, t))\}, \quad (9)$$

and it has the desired properties. In an uncongested region of time-space where both  $K$  and  $k$  are below  $k^0$  the right side of (9) is  $T(K(x, t))$ ; i.e., it reduces to (7a). Similarly, in a congested region where  $(K, k) > k^0$  the right side of (9) becomes (7b).

The functions  $T$  and  $R$ , respectively specify the maximum flow that can be sent or received by a cell. Thus, Eq. (9) states that the outflow of a cell is the largest value that does not exceed the amount that can be sent by the cell or received by its downstream cell.

The FDE resulting from (6b) and (9) should work well under all kinds of initial conditions; in particular, we should expect the result of (6b) always to be in the range  $[0, k^j]$ . This is always the case for our  $T$  and  $R$  if  $\epsilon$  and  $d$  satisfy the aforementioned cell size condition,  $d \geq v^f \epsilon$  but not otherwise.<sup>1</sup>

We claim that iteration of (6b) and (9) is a first order approximation to the LWR solution that can be run across shocks and discontinuities. As a prelude to the more complete discussion of Sections 4 and 5, the following subsection proves that these claims hold true in regions of the  $(t, x)$  plane where  $S_k(K)$  is constant; e.g., in the special case where  $S(k)$  is piece-wise linear.

### 3.1. Dependence on initial conditions

Here we consider a point  $P$  with coordinates  $(x, t)$ , whose characteristic emanates from an initial point where the density is smooth. We also assume that the point is embedded in a region of the  $(t, x)$  plane where  $S_k(K)$  is constant. Let us also assume for now that  $S_k(K) < 0$ .

In that case, iteration of (6b) leads to an influence diagram as in Fig. 1B, where it can be seen the value of the density at each point is the following weighted average of the two prior values at  $x$  and  $x + d$ :

$$\begin{aligned} K(x, t) &= K(x, t - \epsilon) + (\epsilon/d)[S(K(x, t - \epsilon)) - S(K(x + d, t - \epsilon))] \\ &= (1 - p)K(x, t - \epsilon) + pK(x + d, t - \epsilon) \end{aligned}$$

<sup>1</sup>To demonstrate that  $K \leq k^j$  it suffices to show that  $K(x, t)/\epsilon + Q(x - d, t)/d \leq k^j/\epsilon$ , or that—by virtue of (9)— $K(x, t)/\epsilon + R(k^j - K(x, t))/d \leq k^j/\epsilon$ . This will be true if  $R(z) \leq zd/\epsilon$ , which holds because we have specified that  $v^f \leq d/\epsilon$  and we know that  $R(z)/z \leq v^f$ . The latter inequality holds because the left side is the mean of  $R'$  in  $(0, z)$ , and  $v^f$  bounds  $R'$ . To demonstrate that  $K \geq 0$  it suffices to show that  $K(x, t)/\epsilon \geq Q(x, t)/d$ ; i.e.,  $K(x, t)/\epsilon \geq T(K(x, t))/d$ . This, again, is satisfied if  $T(z)/z \leq v^f$ , which also holds for all  $z$ .

where  $p$  denotes the (positive) wave speed expressed in the following dimensionless form:  
 $p = |S_k| \epsilon / d \leq 1$ .

One more iteration yields:

$$K(x, t) = (1 - p)^2 K(x, t - 2\epsilon) + 2p(1 - p)K(x + d, t - 2\epsilon) + p^2 K(x + 2d, t - 2\epsilon).$$

As the process is repeated, we find that the weights of the densities at any prior time  $t'$  continue to be the terms in the binomial expansion of  $[(1 - p) + p]^{(t - t')/\epsilon}$ . This means that  $K(x, t)$  can be expressed as the expectation of  $K(x + id, 0)$ , where the number of lattice points upstream,  $i$ , is viewed as a binomial random variable arising from  $t/\epsilon$  Bernoulli trials with probability of success,  $p$ .

We note that the mean of  $i$  is  $pt/\epsilon$ , which corresponds to the location of the source of the characteristic passing through  $P$ :  $x_o = x - S_k t$ . We also note that the standard deviation of  $i$ ,  $[(1 - p)pt/\epsilon]^{1/2}$ , translates to  $[(1 - p)pd^2 t/\epsilon]^{1/2}$  length units, which vanishes as  $(d, \epsilon) \rightarrow 0$  in a fixed ratio. Thus, the bulk of the contribution toward  $K(x, t)$  comes from a narrow range of locations centered around the source of the characteristic passing through  $P$ , and this range approaches zero with the  $1/2$  power of the lattice spacing. The same result is obtained for forward moving waves.

Because the only significant weights are at locations that are arbitrarily close to  $x_o$ , the predicted density at  $P$  approaches the actual density at the source of the characteristic, i.e., the LWR density at  $P$ , as  $(\epsilon, d) \rightarrow 0$  in a fixed ratio. And furthermore, the presence of a shock (or an unstable discontinuity) near  $P$  can have no effect on the predictions, as  $(\epsilon, d) \rightarrow 0$ .

An expression for the error in the approximation is obtained from the difference between the expectation of a 2<sup>nd</sup> order power series expansion of the initial density profile about the source of the characteristic and the value of the density at said source. If we use “ $E$ ” for the statistical expectation operator and let  $k_{ox}$  and  $k_{oxx}$  denote the first and second derivatives of  $k(x, 0)$  at said source,  $x = x_o$ , we can write for the error in  $K$  (as  $(d, \epsilon) \rightarrow 0$  in a fixed ratio):

$$\begin{aligned} K(x, t) - k(x_o, 0) &\approx E\{k(x_o, 0) + k_{ox}(x - x_o) + \frac{1}{2}k_{oxx}(x - x_o)^2\} - k(x_o, 0) \\ &= E\{\frac{1}{2}k_{oxx}(x - x_o)^2\} = \frac{1}{2}k_{oxx}p(1 - p)d^2 t/\epsilon. \end{aligned} \quad (10)$$

In agreement with the results in Daganzo (1994), which found no error growth with  $t$  for a  $S(k)$  relation where the wave speed was either 0 or 1, this expression indicates that errors are minimal when  $p$  is either zero or 1 and greatest when  $p = 1/2$ .

The expression also indicates that errors are proportional to the lattice spacing, to the time elapsed and to the curvature of the initial density profile. The reader can check that (10) is true by applying the FDE to the following simple data,  $k(x, 0) = 50 + x^2/2$  veh/mile and  $S(k) = \min\{k, (250 - k)/4\}$  veh/min, to predict the density along any characteristic; e.g., the one with source at  $x_o = 10$ . For this choice the exact result is  $k = 100$  veh/mi. With  $d = 1$  mile and  $\epsilon = 1$  min, the wave backs up one cell spacing for each 4 clock ticks ( $p = 1/4$ ) and exact readings of the density can be taken every 4 ticks. After 4 and 8 ticks the algorithm yields  $K = 100.375$  and 100.75, respectively, displaying an error that is in precise coincidence with Eq. (10). This good fit is not fortuitous; under our assumptions, Eq. (10) is exact if  $k(x, 0)$  is quadratic in the domain of dependence of the point in question.

#### 4. ACCURACY OF THE FDE

This section describes quantitatively the difference between the solution produced by the FDE and the exact one for general, smooth  $S(k)$ 's. It is shown that to a second order accuracy in  $(d, \epsilon)$  the error,  $\Theta$ , introduced at each step of the procedure is given by:

$$\Theta = \frac{1}{2}p(1 - p)K_{xx}d^2 \pm [p - \frac{1}{2}]S_{kk}(K_x)^2\epsilon d,$$

and that the accumulation of these errors along a characteristic can be reduced to an expression, Eq. (14) below, that only involves the local properties of the initial density profile,  $k(x, 0)$ , at the source of the characteristic, as in Eq. (10). The reader may skip the somewhat dry material leading to Eq. (14) without loss of continuity.

In the exact theory, the solution at time  $t + \epsilon$  is obtained from the solution at time  $t$  by:

$$k(x, t + \epsilon) = k(x - S_k\epsilon, t)$$

where  $S_k$  is evaluated for the density prevailing at  $(x - S_k\epsilon, t)$ .

In a region where  $K < k^0$  (or  $K > k^0$ ), the FDE recursion can be expressed in terms of  $K$  alone in the following manner:

$$K(x, t + \epsilon) = K(x - S_k\epsilon, t) + [K(x, t) - K(x - S_k\epsilon, t)] \\ \pm (\epsilon/d)[S(K(x, t)) - S(K(x \pm d, t))]$$

where the “+” sign holds if  $S_k < 0$  and the “-” sign if  $S_k > 0$ .

If  $K(x, t)$  is smooth the terms in brackets can be expressed to a second order accuracy in  $\epsilon$  and  $d$  through a power series expansion about  $(x - S_k\epsilon, t)$  and the above becomes:

$$K(x, t + \epsilon) = K(x - S_k\epsilon, t) - \frac{1}{2}K_{xx}[\epsilon^2 S_k^2 \pm S_k\epsilon d] - [S_k\epsilon/d \pm \frac{1}{2}]S_{kk}(K_x)^2\epsilon d \quad (11)$$

where the “+” signs holds if  $S_k < 0$  and the “-” sign holds otherwise. This convention is applied in the formulas that follow.

Because the first term on the right side of (11) is the LWR solution, the last two terms capture the error introduced by the FDE approximation. Using  $p = |S_k|\epsilon/d$ , we can express this error (i.e., the error committed in time  $\epsilon$ ) as:

$$\Theta = \frac{1}{2}p(1 - p)K_{xx}d^2 \pm [p - \frac{1}{2}]S_{kk}(K_x)^2\epsilon d. \quad (12)$$

Before quantifying the effect of (12) we note that the new solution should be close to the exact LWR solution because the approximation only introduces a small diffusion-like effect. To see this, note that the last term of (11) can be eliminated by evaluating  $S_k$  in the first term at a displaced location, i.e., at  $x - [S_k\epsilon/d \pm \frac{1}{2}]d$ , so that (11) can be interpreted as a superposition of two effects: a kinematic wave effect (as in 11), captured by the first and third terms, and a diffusion effect captured by the second term; i.e., the first term of (12). Therefore, Eq. (11) will be stable if the diffusion coefficient of (12) is positive; i.e., if  $p \leq 1$  for all  $S_k$ . This happens if the cell length restriction specified in Section 3,  $d \geq \epsilon v^f$ , is satisfied.

Qualitatively, the solution of (11) is similar to the solution without the diffusion term in time-space regions where the characteristics diverge (e.g.,  $K_x$  negative for concave  $S(k)$ ). In such regions the kinematic waves will tend to smooth out the density as does the diffusion term. The effect of the latter, however, declines as the curvature of the density profile approaches zero, whereas the kinematic wave effect continues to be felt. When the kinematic waves converge (e.g.,  $K_x$  is positive for concave  $S(k)$ ), the kinematic waves tend to increase  $|K_x|$  (eventually forming a shock in the LWR theory) whereas the diffusion term tends to smooth out the density profile. We would expect an equilibrium between these two effects to be reached in the vicinity of a shock, so that in the FDE the shock would appear as a rapid variation in density. Section 5 describes the structure of this profile.

The error in the FDE predictions along a characteristic passing through  $x_0$  at time  $t = 0$  can be evaluated as the line integral of  $\Theta/\epsilon$  along the characteristic. Because  $\Theta$  involves the unknowns  $K_x$  and  $K_{xx}$ , they can be approximated by the (known)  $k_x$  and  $k_{xx}$  in as much as  $K$  and its derivatives converge to  $k$ . In the LWR solution, the latter are



given by the following simple functions of the initial conditions at the source of the characteristic,  $k_o$ ,  $k_{ox}$ ,  $k_{oxx}$ ,  $S_{okk}$ , and  $S_{okkk}$ :

$$k_x = k_{ox}/D \text{ and } k_{xx} = k_{oxx}N/D^2, \quad (13a)$$

where  $D$  and  $N$  are the following functions of time:

$$D = 1 + S_{okk}k_{ox}t, \text{ and} \quad (13b)$$

$$N = 1 - S_{okkk}(k_{ox})^3/(k_{oxx}t). \quad (13c)$$

Expression (13a) for  $k_x$  is simply the ratio of the first difference in  $k$  along neighboring characteristics for a given  $t$ , and the separation between the characteristics at time  $t$ . To see this recall that  $k$  remains constant along any characteristic and therefore so does the first difference in  $k$ :  $k_{ox}dx$ . Thus, the formula for the ratio must be proportional to the reciprocal of the separation between the characteristics, which varies with time as  $Ddx$  with  $D$  given by (13b). (This should be clear after noting that characteristics separated by distance  $dx$  at time  $t = 0$  will have slopes in the  $(t, x)$  plane given by  $S_{ok}$  and  $S_{ok} + S_{okk}k_{ox}dx$ ; thus, their separation at time  $t$  is  $dx + S_{okk}k_{ox}tdx = Ddx$ , as stated.) Similar considerations involving second differences yield the expression for  $k_{xx}$ .

Note that the denominators in (13a) would vanish at the time when neighboring characteristics would cross, but in the LWR solution this can only happen at the singular point where a shock would first form. (The reader may recognize that the formula in Lighthill and Whitham, 1955, for the time to formation of a shock is obtained by setting  $D = 0$ .)

Using (13) in the expression for  $\Theta$  and integrating  $[\Theta/\epsilon]$  from 0 to  $t$ , we obtain the following result:

$$(td/D)[\frac{1}{2}F(pd/\epsilon)(1 - p)k_{oxx} \pm (p - \frac{1}{2})S_{okk}(k_{ox})^2], \quad (14)$$

where the factor  $F$  is given by:

$$F = S_{okkk}(k_{ox})^3/k_{oxx} + [(1 + D)/(2D)][1 + S_{okkk}(k_{ox})^2/(S_{okk}k_{oxx})]$$

If  $S$  is quadratic at  $k_o$  ( $S_{okkk} = 0$ ), then  $F$  reduces to:

$$F = [(1 + D)/(2D)].$$

Equations (14) are an asymptotic approximation for the error in the FDE. Although the method of derivation was different, we note that (14) is consistent with the backward induction result of Section 3.1; i.e., for the characteristics of piecewise linear  $S(k)$  relations (where  $S_{okkk} = S_{okk} = 0$  and  $D = F = 1$ ) Eq. (10) is recovered.

Although (14) is only an asymptotic approximation for small  $d$ , it seems to be accurate enough to predict order of magnitude errors when the lattice size is not infinitesimal. To illustrate this, the FDE is applied to the initial density profile of the example in Section 3.1 after introducing substantial curvature in the  $S(k)$  relation with the new formula:  $S(k) = k$  veh/min if  $k \leq 50$  veh/mile, and  $S(k) = k(250 - k)/200$  if  $50 < k \leq 250$ . Predictions made after 4 steps of the procedure for the characteristic with  $k_o = 150$  veh/mi, with  $(d, \epsilon) = 1, 0.5, 0.25, 0.1$ , and  $0.01$  (mi, min), can then be compared with the predictions of Eq. (14). The input data for (14) are  $p = 0.25$ ,  $S_{okk} = -0.0025$ ,  $S_{okkk} = 0$ ,  $k_{ox} = 200\frac{1}{2}$  and  $k_{oxx} = 1$ . The following Table 1 summarizes the results.

In our limited experience the predictions appear to be even more accurate for characteristic emanating from the interfaces between cells; (as expected) the accuracy improves for  $\epsilon \rightarrow 0$ .

The foregoing arguments only relied on the smoothness of  $K(x, t)$  and  $k(x, t)$  along

Table 1. Errors in the prediction of density ( $k = 150$ ) for different discretizations

$\epsilon$	Eq. (14)	Actual
1	1.02	1.10
0.5	0.235	0.245
0.25	0.0567	0.0579

the characteristic. Therefore, Eq. (14) applies even if the initial data includes discontinuities such as shocks. However, the expression cannot be applied to points on a fan of characteristics issued from an unstable discontinuity because  $k(x, 0)$  is not smooth at  $x_0$  in this case. For concave  $S(k)$ , an informal qualitative argument in agreement with our limited practical experience (and with the result of Section 3.1) suggests that the proposed FDE method also approximates the physically relevant solution in this case.

Starting with a small  $d$ , one can approximate the initial density profile within a neighborhood of  $x_0$  by a step function with upstream densities at the lattice points equal to  $k^u$  and downstream densities equal to  $k^d$ . Consideration of (6b) and (9) reveals that the approximation at the lattice points  $K(x_0 + id, \tau\epsilon)$  (where  $i$  and  $\tau$  are integers) is only a function of  $i$  and  $\tau$  that is monotonic with respect to  $i$  and becomes smooth as  $\tau$  increases—for concave  $S(k)$ . Once the differences  $[K(x, \tau\epsilon) - K(x - d, \tau\epsilon)]$  have become small, for a sufficiently large  $\tau$ , the finite difference recursion can be approximated to high accuracy by (11). By choosing  $\tau d \rightarrow 0$ , the kinematic waves in the original and new PDEs will originate in the vicinity of  $x_0$  and the two PDE solutions will resemble each other.

## 5. THE SHOCK PROFILE

We now describe the shock capturing properties of the FDE approximation, with particular attention to the number of lattice points that it takes for a given percentage of the variation in density across the shock to take place. This is done for the important case where  $S$  is concave; background derivations are provided in the appendix.

We consider the special case where the downstream and upstream densities on both sides of the shock,  $k^d$  and  $k^u$  are constant, but the results extend to variable densities for sufficiently fine mesh sizes. This is true because, as is explained in the appendix, the number of steps to equilibrium is independent of  $\epsilon$  and, thus, the time to reach equilibrium vanishes as  $\epsilon \rightarrow 0$ .

Consider first a case where the waves propagate in different directions on both sides of the shock (i.e.,  $k^d > k^o > k^u$ ). Figure 3, depicts by means of a dark slanted line a shockpath that moves with positive velocity. (Because in the FDE, the shockpath may span many lattice points, it is defined here as the line that separates points with  $K > k^o$  from points with  $K < k^o$ .) Arrows in this diagram represent dependence, meaning that the value of  $K$  at the source of an arrow influences the value at its end. Note that, away from the shock, the displayed pattern is consistent with our prior discussion of Fig. 1. The only discrepancy with what we have seen occurs near the slanted line, where some dotted arrows denoting possible dependences are displayed. Consideration of Eqs. (6b) and (9) reveals that at any given time, two crossing arrows emanate from the pair of points straddling the shockpath, as shown in the figure. And furthermore, only one of each pair of crossing arrows materializes—the specific one being determined by the relative values of  $K$  at the two origin points.

Given the geometry of dependence in Fig. 3, it should be clear that every downstream point that is separated from the shock path by at least one intervening lattice point (e.g., point  $P$  in the figure) will have a domain of dependence at time  $t = 0$  that will be entirely downstream of the shock (see Fig. 1). Therefore,  $K$  will equal  $k^d$  at all such points (e.g.,  $P, P_1, P_2$ , etc. . .). This means that the transition from  $K = k^d$  to  $K < k^o$  (e.g., to point  $Q$  below the shockpath) is achieved abruptly in two cells.

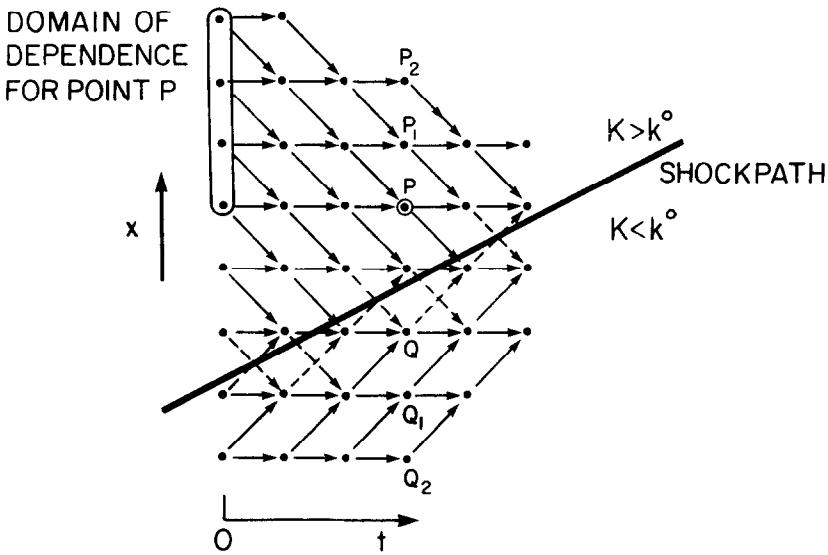


Fig. 3. Influence diagrams and shocks.

As we move away from the shock on its upstream side the domain of dependence of successive lattice points (e.g.,  $Q$ ,  $Q_1$ ,  $Q_2$ , etc. . .) changes gradually and includes points on both sides of the shock. Because the determining data changes gradually for this sequence of points, one would expect  $K$  to decline gradually toward  $k^u$ . The figure reveals that this transition can take up to  $|Ut/\epsilon|$  cells.

The same conclusions are reached if the shock moves with negative velocity, except now the abrupt transition is upstream of the shock between  $k^u$  and  $K > k^o$ ; as in the previous case, this occurs on the side of the shock where the waves travel in the opposite direction as the shock.

If the waves forming the shock travel in the same direction (i.e.,  $k^d > k^u > k^o$ , or  $k^o > k^d > k^u$ ) then the influence diagram is identical on both sides of the shock, with a domain of dependence that includes only downstream cells or only upstream cells for every point on the lattice and the resulting predictions vary gradually on both sides.

The appendix shows that the equilibrium shock velocity in the FDE satisfies (5), and that the width of the shock profile (between any two intermediate densities  $k^a$  and  $k^b$ ) is of order  $d$ ; thus, it can be measured as the number of cells. Approximate formulas are given. For the two wave velocity model, Eqs. (A4) and (A5) in the appendix predict that whenever  $U > 0$ , 99% of the shock is covered with four cells or less. More cells are needed for negative  $U$ s, and the number tends to infinity as  $U$  approaches the negative wave velocity. Both of these observations are consistent with our experience with the model. The latter phenomenon was discussed in Daganzo (1994), where a modification to the FDE was suggested to increase focusing.

As an example, Fig. 4 displays the evolution of the FDE shock for a hypothetical case where in an unspecified system of units:  $S(k) = k - k^2/2$  (and  $k^o = 1$ ). At  $t = 0$ , the density is assumed to increase linearly between  $k^d = 0.2$  and  $k^u = 1.3$  between  $x = 0$  and  $x = 11$ , as shown by the slanted line in Fig. 4. For  $\epsilon = d = 1$ , the remaining lines show the FDE shock profile for  $t = 5, 10, 15, 20$ , and  $36$ . It can be seen in Fig. 4 that the shock reaches an equilibrium and that thereafter it moves with velocity:  $(16-12)/(36-20) = 0.25$ , as predicted by (5). Although the resolution of the figure masks the fact, the shock, as expected, ends abruptly downstream and gradually upstream.

The size of the jump in density across the two cells spanning the center of a shock (if as shown in Fig. 5 we define the center as the point  $k^c$  where  $S_k(k)$  is closest to  $U$ ) can be crudely approximated from the reciprocal of the integrand in appendix equations (A4) and (A5) evaluated at  $K = k^c$ ; i.e., if we choose  $d = \epsilon v^f$  and use  $u = U/v^f$ , the jump,  $J$  satisfies the relation:

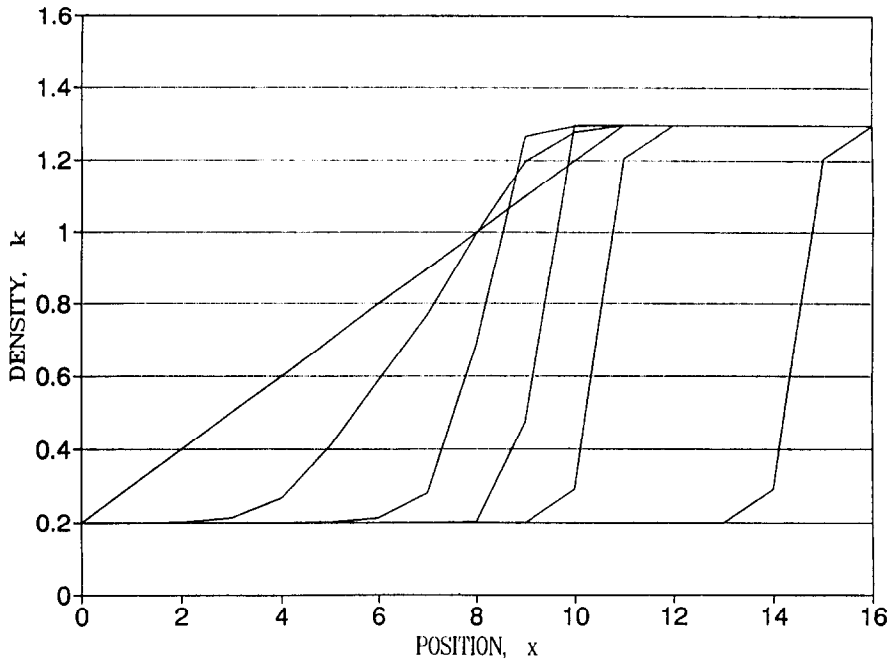


Fig. 4. Example of shock evolution in the FDE.

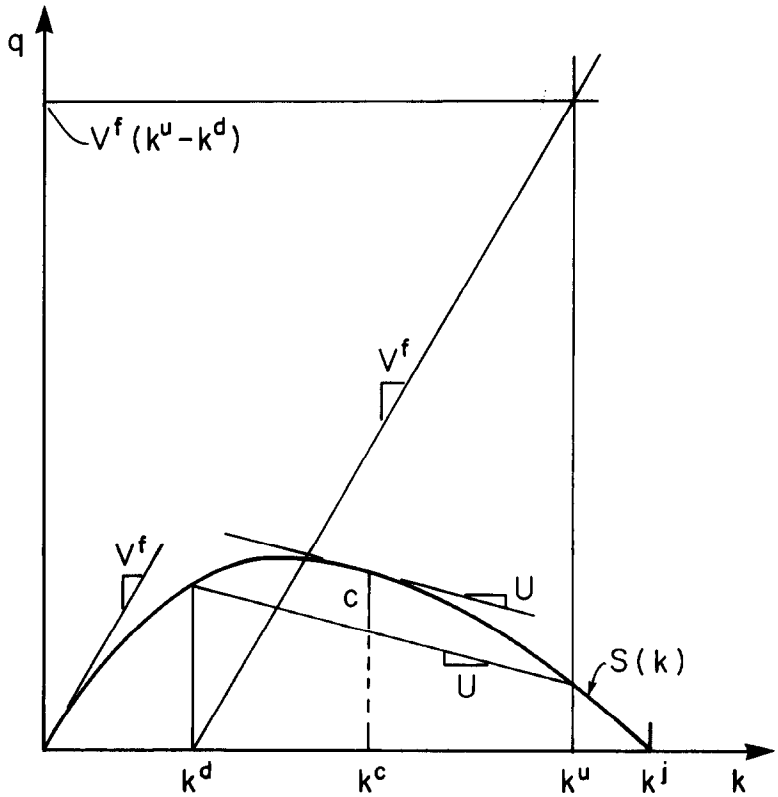


Fig. 5. Graphical approximation of the cell occupancy jump across the center of a shock.

$$Jv^f \approx 2c/[(1 - |u|)|u|], \quad (15)$$

where  $c$  is the length of the chord identified in Fig. 5. The right side of (15), which is always greater than  $8c$ , can be compared at a glance with  $v^f(k^u - k^d)$ ; see Fig. 5. If (15) is comparable or greater than  $v^f(k^u - k^d)$ , as happens in Fig. 5, this simply means that the bulk of the shock transition will be concentrated in one or two cells. This result should not be surprising: large differences in slopes at the ends of the chord mean greatly focused characteristics which can overcome the diffusion effect of the FDE over short distances and this results in quick transitions. Similar slopes mean longer transitions.

It can also be seen from appendix Eqs. (A4) and (A5) that the shock tail must decrease exponentially—on the side(s) where the waves run with the shock. More specifically, the number of cells between  $k^a = k^d + \delta$  and  $k^b = k^d + \delta'$  (for small  $\delta$  and  $\delta'$  and  $U > 0$ ) is approximately:

$$I = C \ln(\delta/\delta'), \quad (16a)$$

where

$$C = (\epsilon/2d)[U^2 - (2U - d/\epsilon)S_k(k^d)]/[U - S_k(k^d)]. \quad (16b)$$

The expression:

$$C = (\epsilon/2d)[U^2 - (2U + d/\epsilon)S_k(k^u)]/[U - S_k(k^u)] \quad (16c)$$

holds when  $U < 0$ .

The results in this section and the appendix have shown that the shock profile in the proposed FDE approximation reaches an equilibrium for any equation of state that is strictly concave. Because the number of cells needed to include any percentage of the shock is independent of the lattice, the shock can be made arbitrarily sharp by using finer meshes.

## 6. EXTENSIONS

We assumed in Sections 4 and 5 that the  $S(k)$  relation was smooth, but the results extend to continuous and piecewise differentiable equations of state, such as those proposed in Newell (1993). This should be rather obvious, because any piecewise differentiable  $S(k)$  relation can always be represented as the limit of a sequence of smooth relations and the limit of the sequence of solutions solves the  $S(k)$  problem. The results in Daganzo (1994) for a trapezoidal relation confirm this.

It was assumed in Sections 3 to 5 that the proposed FDE was applied to an initial value problem, where the system's conditions are specified at time  $t = 0$  for all  $x$ . With simple modifications, the algorithm can be applied to other boundary condition problems (e.g., to a finite highway with given input flow and output flows, assuming they are well-posed.) The arguments leading to (14) could then be repeated, to obtain a similar error formula in terms of the derivatives of  $k$  along the boundary (e.g., with respect to time at the fixed location of a boundary for the finite highway case). Although the form of the dependence on time and the lattice spacing should be analogous, the variable " $t$ " in the new formula would have to be interpreted as the time interval between the point in question  $(t, x)$  and the source of its characteristic on the boundary  $(t_o, x_o)$ . Then, whenever  $t - t_o$  is bounded, as in the typical finite highway problem, convergence may be uniform.

The results of the previous section can also be extended to the inhomogeneous highway (e.g., with varying width and time-dependent conditions). The only (reasonable) requirements we impose when conditions change with time are: (a) that the free-flow speed at any location is bounded (i.e., it should not exceed a value,  $v^f$ , which should be used to define the mesh dimensions) and (b) that the jam density  $k^j$  should not be allowed to drop below the current density.

Although the derivations of Sections 4 and 5 could be repeated for the inhomogeneous highway, it should be sufficient (and easier) to note that any space-inhomogeneities arising in real life are approximated by a piecewise homogeneous highway, and that the results of Sections 3 to 5 apply to the homogeneous pieces of such highway. (A similar argument holds for time-varying conditions.)

An extension to multideestination networks is also possible after careful consideration of the boundary conditions that one would impose at the boundaries between links. This has already been done for trapezoidal  $S(k)$  relations (Daganzo, 1995), with examples given in Daganzo and Lin (1993). The modifications needed to extend these results to general  $S(k)$  curves with general sending and receiving functions are simple.

## 7. DISCUSSION

This article has shown that the kinematic wave PDE model is approximated by a FDE, and has also shown that the counterintuitive behavior of other FDEs is an intrinsic property of the FDEs and not of the LWR model. By now, it should be evident that discretizing a PDE on a lattice, even when the PDE solution is smooth, does not guarantee a proper solution; a more careful analysis is needed.

If the error analysis of Sections 3 and 4, for the case with  $S_{kk} = 0$ , is repeated for the centered difference method of Lax (1954) we find a larger error than given by (10):

$$\frac{1}{2}k_{xx}[p(1 - p) + 1]d^2t/\epsilon.$$

Better accuracy, however, is not the main attraction of the proposed FDE. Unlike the Lax method (and more complicated second-order methods) the proposed FDE never moves vehicles back. As such, it retains a fidelity to real life that is attractive in practical engineering applications where the lattice cannot be made arbitrarily small. The proposed FDE formalizes the intuitive concept (introduced by others in the past; e.g., Sheffi et al., 1982; Chang et al., 1985; Algadhi & Mahmassani, 1990) that traffic flow can be described as a natural competition between the vehicles that want to move forward (from a cell to the next) and those that are allowed to move by the congested cell ahead. Prior models, however, do not perform satisfactorily under all conditions. It is the introduction of the precise "sending" and "receiving" functions of Eq. (8) that corrects this deficiency.

In unrelated parallel work, Bui et al., (1992) have proposed another FDE approximation (Godunov, 1961) to model the homogeneous freeway (see also, LeVeque, 1992). Our proposed FDE, with sending and receiving functions, can be shown to be a streamlined member of Godunov's family. As a result, the results in this article also demonstrate the convergence, accuracy, and shock capturing properties of Godunov's family under the general conditions that arise in traffic problems.

*Acknowledgement*—I thank Gordon F. Newell for the many discussions over the last few years, in which he shared his vast knowledge on the subject matter pertaining to this article. The comments of two anonymous reviewers are also gratefully acknowledged.

## REFERENCES

- Algadhi, S., & Mahmassani, H. (1990). Modeling crowd behavior and movement: Application to Makkah pilgrimage. In *Transportation and Traffic Theory* (pp. 59–78). (M. Koshi, ed.), Proceedings 11th International Symposium on Transit and Traffic Theory. Yokohama, Japan. New York: Elsevier.
- Bick, J. H., & Newell, G. F. (1960). A continuum model for two-directional traffic flow. *Q. App. Math.*, 18(2) 191–204.
- Bui, D. D., Nelson, P. & Narashimhan, S. L. (1992). Computational realizations of the entropy condition in modeling congested traffic flow. *Federal Highway Administration report FHWA/TX-92/1232-7*.
- Chang, G., Mahmassani, H., & Herman, R. (1985). A macroscopic traffic simulation model to investigate peak-period commuter decision dynamics. *Transportation Research Record*, 1005, 107–121.
- Cremer, M., & May, A. D. (1985). An extended traffic model for freeway control. *Research Report UCB-ITS-RR-85-7*. Berkeley, CA: Institute of Transportation Studies, University of California.
- Daganzo, C. F. (1995). The cell transmission model. Part II: Network traffic. *Transportation Research*, 29B, 79–94.

- Daganzo, C. F. (1994). The cell-transmission model: A dynamic representation of highway traffic consistent with the hydrodynamic theory. *Transportation Research*, 28B, 269–288.
- Daganzo, C. F., & Lin, W. H. (1993). Moving queues in traffic networks. In *Large Urban Systems* (pp. 121–136). (Yagar, S., & Santiago, A., eds.), *Proc. Advanced Traffic Manag. Conf.*, St. Petersburg Beach, FL. Washington, DC: FHWA.
- Godunov, S. K. (1961). Bounds on the discrepancy of approximate solutions constructed for the equations of gas dynamics. *J. Com. Math. and Math. Phys.*, 1, 623–637.
- Lax, P. D. (1954). Weak solutions of nonlinear hyperbolic equations and their numerical computations. *Commun. Pure App. Math.*, 7, 159–193.
- LeVeque, R. J. (1992). *Numerical methods for conservation laws (2nd ed.)*. Lectures in Mathematics ETH Zürich, Birkhäuser Verlag, Basel, Switzerland.
- Lighthill, M. J., & Whitham, J. B. (1955). On kinematic waves. I Flow movement in long rivers. II A theory of traffic flow on long crowded roads. *Proc. Royal Soc. A*, 229, 281–345.
- Luke, J. C. (1972). Mathematical models for landform evolution. *Journal of Geophysical Research*, 77, 2460–2464.
- Michalopoulos, P. G., Beskos, D. E., & Lin, J. K. (1984). Analysis of interrupted traffic flow by finite difference methods. *Transportation Research*, 18B, 409–421.
- Michalopoulos, P. G., Beskos, D. E., & Yamauchi, Y. (1984a). Multilane traffic flow dynamics: Some macroscopic considerations. *Transportation Research*, 18B, 377–396.
- Munjal, P. K., & Pipes, L. A. (1971). Propagation of on-ramp density perturbations on unidirectional two- and three-lane freeways. *Transportation Research*, 5, 241–255.
- Newell, G. F. (1989). Comments on “Traffic dynamics.” *Transportation Research*, 23B(5), 386–391.
- Newell, G. F. (1993). A simplified theory of kinematic waves in highway traffic, Part I: General theory; Part II: Queuing at freeway bottlenecks; Part III: Multi-destination flows. *Transportation Research*, 27B(4), 281–314.
- Payne, N. J. (1971). Models of freeway traffic and control. *Math. Models Publ. Sys., Simul. Council Proc.*, 28(1), 51–61.
- Payne, H. J. (1979). FREFLO: A macroscopic simulation model of freeway traffic. *Transportation Research Record*, 722, 68–77.
- Richards, P. I. (1956). Shockwaves on the highway. *Opns. Res.*, 4, 42–51.
- Sheffi, Y., Mahmassani, H., & Powell, W. B. (1982). A transportation network evacuation model. *Transportation Research*, 16A, 209–218.

## APPENDIX

*Profile of the shock tail at equilibrium*

Here, we examine the development and stabilization of a shock when  $K(x,0)$  increases with  $x$ . Initially, we assume that  $K(x,0) < k^0$  in the region of interest so that the shock will have two tails at equilibrium and will move forward with velocity  $U$ . For these conditions we can write from (6b) and (9):

$$K(x, t + \epsilon)/\epsilon = K(x, t)/\epsilon + (1/d)[S(K(x - d, t)) - S(K(x, t))] \quad (A1)$$

If  $K(x - U\epsilon, t)/\epsilon$  is subtracted from both sides and the resulting right side is expressed as a second order power series expansion about location  $x - U\epsilon$ , we find:

$$(K_t)^0 = (u - S_k)K_x + (\epsilon/2)[U^2 - (2U - d/\epsilon)S_k]K_{xx} - (\epsilon/2)(2U - d/\epsilon)(S_{kk})(K_x)^2 \quad (A2)$$

where  $(K_t)^0$  represents the partial derivative of  $K$  with respect to  $t$  in the moving coordinate system traveling with an observer moving with the shock.

If  $S_{kk} = 0$  and  $S_k = U$ , the above expression becomes the heat diffusion equation:

$$(K_t)^0 = \frac{1}{2}[p(1 - p)d^2/\epsilon]K_{xx},$$

where, as in the text, we use  $p$  to represent  $|S_k|\epsilon/d = U\epsilon/d$ . For this special case,  $K$  does not reach an equilibrium as  $t \rightarrow \infty$ . If  $K(x,0)$  is discontinuous at  $x = 0$  then  $K(x,t)$  is given, in the moving coordinate system, by the cumulative normal distribution function with mean zero and standard deviation  $[p(1 - p)d^2t/\epsilon]^{1/2}$ . (This shock spreading phenomenon, reported in Daganzo (1994), is peculiar to the triangular state equation used there for transitions between states on the right side of the diagram.) In the remaining cases, the profile reaches an equilibrium as  $t \rightarrow \infty$ .

A change of scale to cell-transmission units,  $\tau = t/\epsilon$  and  $x' = x/d$ , transforms (A2) into an equivalent form that only depends on  $\epsilon$  and  $d$  through the (fixed) ratio  $d/\epsilon$ . This means that the number of cells between any two densities  $k^a$  and  $k^b$  is independent of mesh size. It follows that an equilibrium is reached instantaneously for  $\epsilon \rightarrow 0$ , as is claimed in the text.

The equilibrium is found by setting the left side of (A2) equal to zero and solving the resulting ordinary differential equation in  $K$ :

$$0 = (UK - S)_x + (\epsilon/2)[U^2K - (2U - d/\epsilon)S]_{xx}. \quad (A3)$$

This equation can be integrated once to yield:

$$C = (UK - S) + (\epsilon/2)[U^2 - (2U - d/\epsilon)S]K_x,$$

where the integration constant must equal  $Uk^d - S(k^d)$  because  $K_x = 0$  when  $K = k^d$ . The other boundary

constraint ( $K_r = 0$  when  $K = k^u$ ) is redundant when  $U$  is given by  $[S(k^u) - S(k^d)]/[k^u - k^d]$  (i.e., Eq. (5) of the text) but otherwise cannot be satisfied. This establishes that the FDE shock moves with the proper speed.

One more integration step after separating variables and then division of both sides by  $d$  to express distance as a number of cells,  $I$ , yields the following expression for the number of cells used in a transition between  $k^a$  and  $k^b$ :

$$I \approx \int_{k^a}^{k^b} (\epsilon/2d) [U^2 - (2U - d/\epsilon)S_k(K)]/[U(k^d - K) - (S(k^d) - S(K))]dK. \quad (A4)$$

This integral converges for strictly convex equations of state but diverges if  $k^a = k^d$  or  $k^b = k^u$ . That is, the shock tail extends to infinity.

The derivation when  $K(x,0) > k^o$  (waves moving backward) parallels the one just presented and it leads to:

$$I \approx \int_{k^a}^{k^b} (\epsilon/2d) [U^2 - (2U + d/\epsilon)S_k(K)]/[U(k^u - K) - (S(k^u) - S(K))]dK. \quad (A5)$$

In the case where  $k^d < k^o < k^u$  the transition between  $k^o$  and  $k^u$  is abrupt if  $U > 0$ . Then (A4) governs the transition between  $k^a$  and  $k^b$  for  $k^d < k^a < k^b < k^o$ . If  $U < 0$ , then the transition between  $k^d$  and  $k^o$  is abrupt and (A5) holds for the transition between  $k^a$  and  $k^b$  when  $k^o < k^a < k^b < k^u$ .